Strain induced change of bandgap and effective mass in silicon nanowires

Daryoush Shiri, Yifan Kong, Andrei Buin, and M. P. Anantram
Nanotechnology Program, Department of Electrical and Computer Engineering, University of Waterloo, 200 University Ave. W, Waterloo, Ontario N2L 3G1, Canada

(Received 25 April 2008; accepted 26 July 2008; published online 22 August 2008)

This work computationally investigates the electromechanical properties of hydrogen passivated silicon nanowires under uniaxial tensile strain. It has been observed that bandgap changes can be as large as 60 and 100 meV per 1% axial strain for [100] and [110] nanowires, respectively. This rate of change in the bandgap is independent of nanowire size and depends only on the growth direction. More importantly, the nature of the bandgap can reversibly change from indirect to direct as a function of strain. It is also observed that for larger diameter nanowires, the indirect-to-direct transition occurs at smaller compressive strain. © *2008 American Institute of Physics*.
[DOI: 10.1063/1.2973208]

Silicon nanowire (SiNW) growth with hydrogen passivation has been demonstrated[1,2] and extensive experimental[3–8] and theoretical[9–11] studies of electronic, optical, and mechanical properties have been performed. SiNWs have a direct bandgap,[2,3,9,10] with potential applications in electronic,[12,13] optoelectronic,[14,15] biomedical, and chemical sensors.[16] Motivated by the aforementioned studies, we have computationally investigated the electromechanical properties of SiNWs.[17] We start with *H*-terminated SiNWs and focus on the experimentally realized[1] [110] growth direction with three different diameters. The total energy of the nanowire structure is minimized by the Tersoff potential.[18] To get the atomic coordinates of a strained nanowire, a small uniform axial compression or expansion ($\alpha < 1\%$) is applied to the nanowire, followed by energy minimization. This task is performed under a constant unit cell volume constraint,[19] where the axial unit cell length is determined by the strain. However the atoms are free to move in all three directions because the radius of the unit cell is larger than the radius of the nanowire. This process is iterated until the desired percentage strain (α) and final unit cell length $P_{new}=P_0(1-\alpha)$ are obtained, where P_0 is the unit cell length of the optimized, unstrained nanowire. The resultant atomic coordinates are then used for bandstructure calculations. The semiempirical $sp^3d^5s^*$ tight binding (TB) method, with Jancu's parameters[20] is used to construct the periodic Hamiltonian in Bloch's equation, and charge self-consistency is neglected.[21]

Figure 1(a) shows the bandgap (E_g) versus strain for the smallest [110] SiNW in our study, which has an average diameter of 1.7 nm. The bandgap decreases linearly with increasing tensile strain ($\alpha > 0$). The linear relationship $E_g(\text{eV})=-0.1\alpha+1.7$, fits the bandgap in the tensile strain region, where the slope is approximately 100 meV/%. In the compressive strain region, the bandgap increases from 0% to −1%, and after −1% it decreases with further increase in strain. More importantly, for a strain larger than −4%, the bandgap becomes indirect, i.e., a direct-to-indirect bandgap transition occurs at −4% strain [Fig. 1(a)]. To understand this transition, the bandstructure is plotted at strains of +1% and −5% in Fig. 1(b). While the bandgap at these two values of strain are comparable, it is clearly seen that the conduction band labeled **L** (light) determines the bandgap at +1% strain while the conduction band labeled **H** (heavy) determines the bandgap at −5% strain. An important consequence of this direct-to-indirect bandgap transition is the different light absorption (with a wavelength equal to the bandgap) at −5%

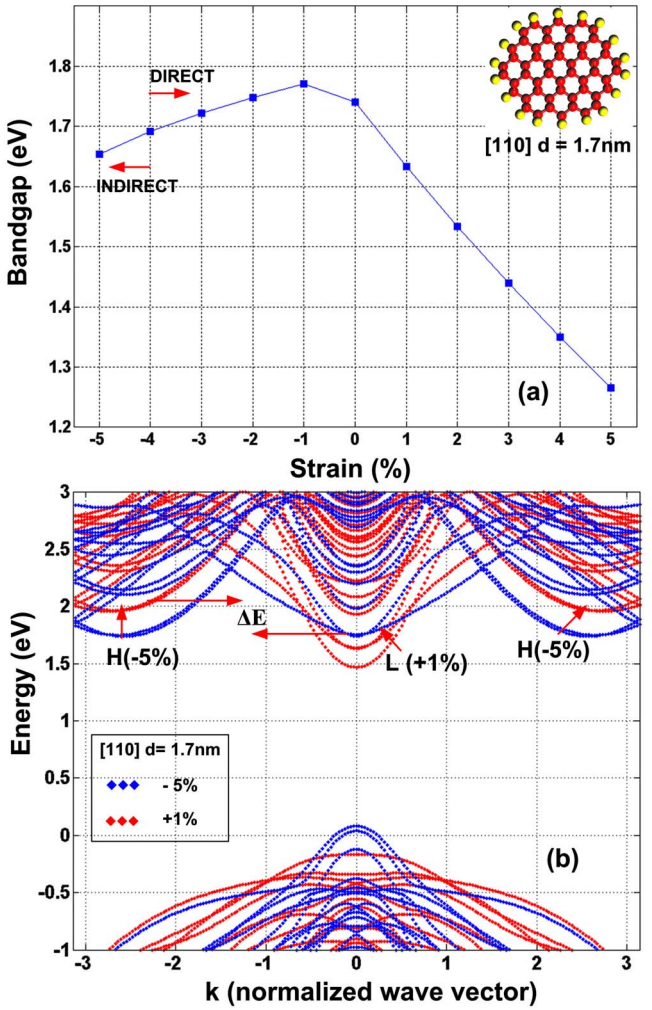


FIG. 1. (Color online) (a) Bandgap vs strain for [110] SiNW with a diameter of 1.7 nm. The bandgap changes linearly with tensile strain and direct-to-indirect transition occurs at −4% strain. Inset shows the cross section of the nanowire where the light and dark atoms are H and Si respectively. (b) Blue (dark) and red (light) curves show that the bandstructure is indirect and direct at −5% and +1% strain.

 © 2008 American Institute of Physics

Downloaded 16 Sep 2008 to 129.97.106.193. Redistribution subject to AIP license or copyright; see http://apl.aip.org/apl/copyright.jsp

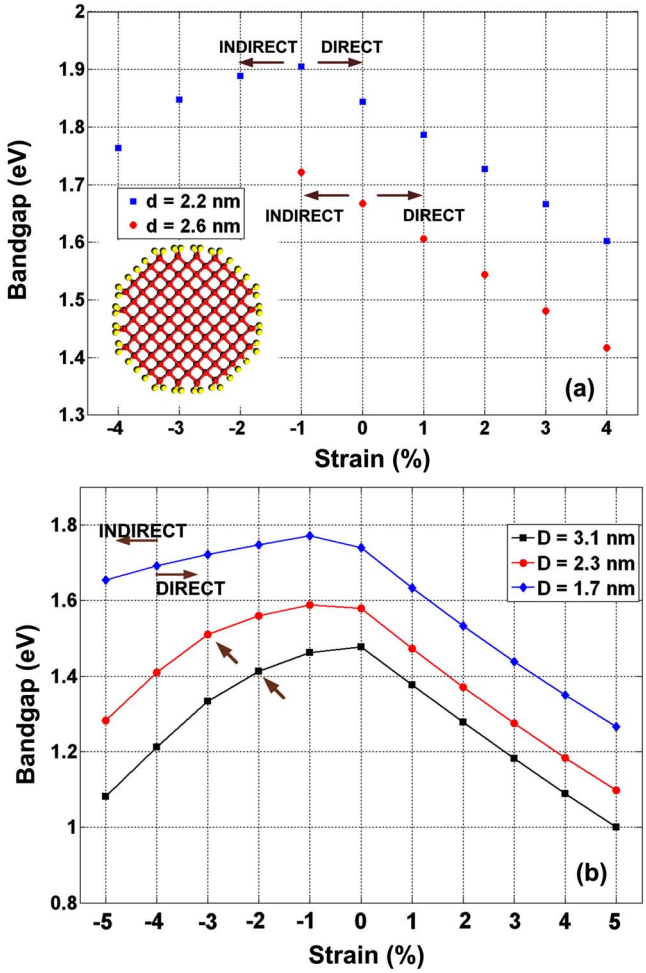


FIG. 2. (Color online) (a) Bandgap vs strain for [100] SiNWs with a diameter of 2.2 nm (square ■). While it shows the same features as Fig. 1(a), the direct-to-indirect transition occurs at a smaller strain of −1%. Circles (●) show the same data for the 2.6 nm diameter [100] SiNW. In this case the bandgap transition point shifts right and occurs at close to the 0% strain. (b) The square (■), circle (●), and diamond (♦) show bandgap vs strain for 3.1, 2.3 and 1.7 nm diameter [110] SiNWs respectively. The direct-to-indirect transition (arrows) occurs at smaller compressive strains as diameter increases.

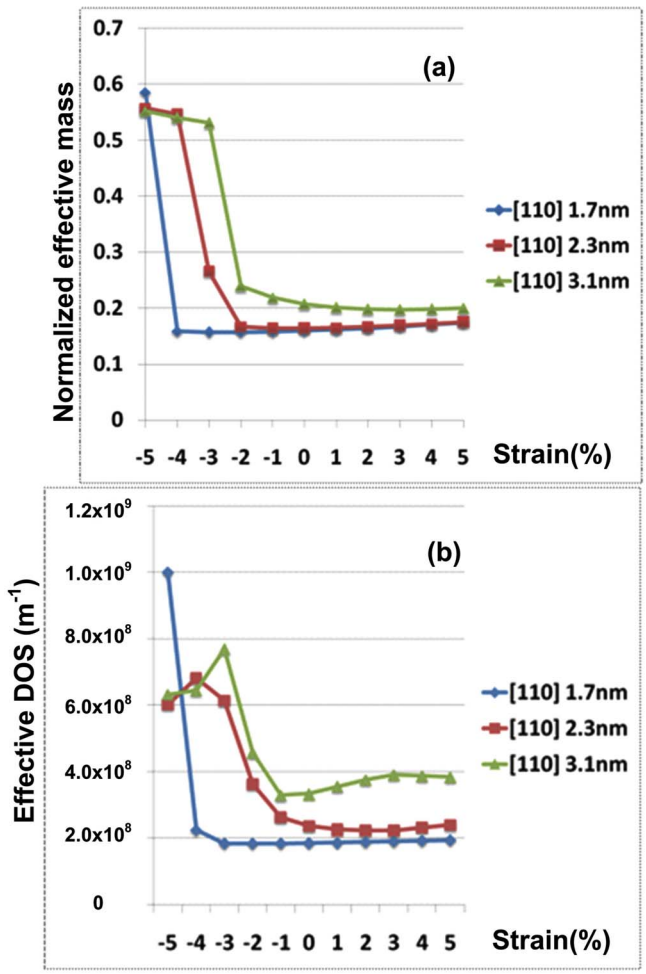


FIG. 3. (Color online) (a) The normalized electron effective mass vs strain for 1.7, 2.3, and 3.1 nm diameter [110] SiNWs. (b) Effective density of states (N_c) vs strain for the same nanowires as (a).

and +1% strain or any two different strain points with equal bandgap values. At −5% strain, optical absorption should be weaker than at +1% strain, because only phonon assisted optical excitation can conserve momentum. In contrast, increased light absorption is expected to occur for the same optical frequency at +1% strain, where the bandgap is direct. The direct-to-indirect transition also exists in a [100] SiNW [Fig. 2(a)]. This nanowire has a diameter of 2.2 nm and the direct-to-indirect transition occurs at a relatively small strain of −1%. The bandgap variation with strain in the tensile region fits the equation $E_g(\text{eV})=-0.06\alpha+1.8$. While the bandgap change with strain is smaller than that of the [110] nanowire, the direct-to-indirect transition with strain is preserved. The generality of bandgap change with strain is further established by comparing the [110] SiNWs with diameters of 1.7, 2.3, and 3.1 nm [Fig. 2(b)]. The features of the electromechanical response remain consistent for all cases considered in Figs. 2(a) and 2(b). For $\alpha>0$, the rate of change of the bandgap with strain is comparable for all nanowires and the direct-to-indirect transition occurs in all three nanowires [Fig. 2(b)].

In comparing with the extensively studied carbon nanotubes (CNTs) case,[22,23] we note that the slope of the bandgap with strain changes rapidly with both diameter and chirality in CNTs,[22] while it is independent of the orientation in the SiNWs considered here. Furthermore, the robust direct-to-indirect transition does not occur in CNTs at the values of strain considered. Also, in comparison to strain engineered bulk heterostructures, the discussion of direct-to-indirect transition is reversible.[24] Experimental verification of our results may be possible by using techniques similar to those used to study the electromechanical properties of CNTs with similar diameters.[7,23]

The physical reason for the decrease in strain with increase in diameter, at which the direct-to-indirect bandgap transition occurs, is that the energy difference between the **L** and **H** bands (ΔE) decreases with increase in nanowire diameter. Quantitatively, this energy difference is 419, 231, and 146 meV for the [110] nanowire with diameters of 1.7, 2.3 and 3.1 nm [Fig. 1(b)]. The conduction band minimum is determined by the **L** (**H**) band when the bandgap is direct (indirect). Increased compressive strain means a smaller energy difference between the minimum of the **L** and **H** bands. This difference becomes zero at the direct-to-indirect transition point and becomes negative after this point. Additionally, the movement of the **L** and **H** bands with strain causes an abrupt change in the conduction band electron effective

Downloaded 16 Sep 2008 to 129.97.106.193. Redistribution subject to AIP license or copyright; see http://apl.aip.org/apl/copyright.jsp

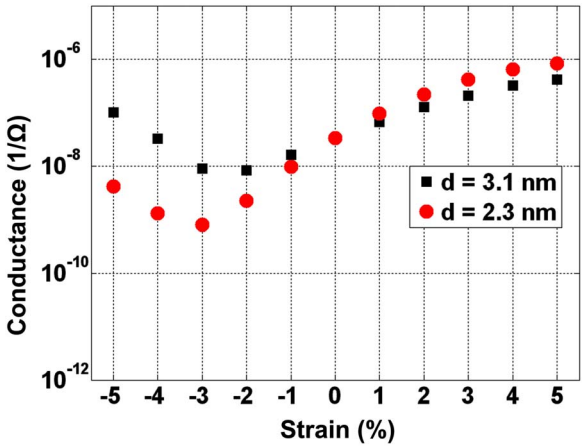


FIG. 4. (Color online) Conductance vs strain is shown for 2.3 and 3.1 nm [110] SiNWs.

mass [Fig. 3(a)]. This occurs at the direct-to-indirect bandgap transition. This is due to the larger mass of the **H** band, which determines the lowest lying conduction band once the bandgap becomes indirect. The change in the mass of the **L** and **H** bands with strain is small [Fig. 3(a)]. The strain dependent effective density of states in the conduction band (N_c) for the [110] SiNW is calculated from:

$$Nc = \sqrt{\frac{2kT}{\pi\hbar^2}} \sum_{i=1}^{N} e^{E_{c\,\min}-E_i/kT} \sqrt{m_i^*},$$

where m_i^* is the effective mass of subband i. E_i and E_{cmin} are the bottom of subband i and the lowest conduction subband. kT and N are thermal energy (26 meV at $T=300$ K) and the number of subbands in the $3kT$ window from E_{cmin}. As shown in Fig. 3(b), the light conduction bands (at $k=0$) primarily contribute to N_c in the tensile strain region. Hence, N_c is smaller in the tensile strain region. The number of eigenstates in the $3kT$ energy window from E_{cmin} increases with the nanowire diameter because the energy level separation associated with quantum confinement decreases. As a result, N_c increases with diameter. The direct-to-indirect bandgap transition corresponds to a peak in N_c because both the heavy (at $k=0$, direct) and light (at $k\neq 0$, indirect) conduction bands contribute to N_c in the $3kT$ window from E_{cmin}. At larger compressive strains, N_c shows a dip, because at strains beyond the direct-to-indirect transition, the heavy (indirect) conduction bands determine N_c and the light conduction bands make an insignificant contribution to N_c. The large change in bandgap and density of states also manifests itself as more than three orders in magnitude change in conductance within the $\pm 2\%$ strain range (Fig. 4).

In summary, we observed that the bandgap of SiNWs can vary by large amounts for a [110] SiNW. The size-independent change can be 100 meV for a 1% strain. We also report a strain induced direct-to-indirect transition in the bandgap,[17] for [110] and [100] SiNW with various diameters. This transition occurs at a strain of 1%–2% for the larger diameters investigated, and hence can be verified experimentally. Accompanying this bandgap transition is an abrupt change in the electron effective mass and density of states. Our results demonstrate that strain-engineered SiNWs are remarkable and point to promise for applications in highly sensitive optical and electromechanical sensors.

This research work was supported by the National Institute of Standards and Technology, Gaithersburg, Maryland. Authors' access to the facilities of the Shared Hierarchical Academic Research Computing Network is acknowledged.

[1] Y. Wu, Y. Cui, L. Huynh, C. J. Barrelet, D. C. Bell, and C. M. Lieber, Nano Lett. **4**, 433 (2004).
[2] D. D. D. Ma, C. S. Lee, F. C. K. Au, S. Y. Tong, and S. T. Lee, Science **299**, 1874 (2003).
[3] J. D. Holmes, K. P. Johnston, R. C. Doty, and B. A. Krogel, Science **287**, 1471 (2000).
[4] J. Kikkawa, S. Takeda, Y. Sato, and M. Terauchi, Phys. Rev. B **75**, 245317 (2007).
[5] T. K. Sham, S. J. Naftel, P. S. G. Kim, R. Sammynaiken, Y. H. Tang, I. Coulthard, A. Moewes, J. W. Freeland, Y. F. Hu, and S. T. Lee, Phys. Rev. B **70**, 045313 (2004).
[6] T. Kizuka, Y. Takatani, K. Asaka, and R. Yoshizaki, Phys. Rev. B **72**, 035333 (2005).
[7] R. He and P. Yang, Nat. Nanotechnol. **1**, 42 (2006).
[8] A. G. Cullis and L. T. Canham, Nature (London) **353**, 335 (1991).
[9] A. Svizhenko, P. W. Leu, and K. Cho, Phys. Rev. B **75**, 125417 (2007).
[10] T. Vo, A. J. Williamson, and G. Galli, Phys. Rev. B **74**, 045116 (2006); J. An Yan, L. Yang, and M. Y. Chou, *ibid.* **76**, 115319 (2007).
[11] M. Menon, D. Srivastava, I. Ponomareva, and L. A. Chernozatonskii, Phys. Rev. B **70**, 125313 (2004); B. Lee and R. E. Rudd, *ibid.* **75**, 041305(R) (2007).
[12] J. Xiang, W. Lu, Y. Hu, Y. Wu, H. Yan, and C. M. Lieber, Nature (London) **441**, 489 (2006).
[13] S. M. Koo, Q. Li, M. D. Edelstein, C. A. Richter, and E. M. Vogel, Nano Lett. **5**, 2519 (2005); Q. Li, X. Zhu, H. D. Xiong, S. Koo, D. E. Ioannou, J. J. Kopanski, J. S. Suehle, and C. A. Richter, Nanotechnology **18**, 235204 (2007).
[14] B. Tian, X. Zheng, T. J. Kempa, Y. Fang, N. Yu, G. Yu, J. Huang, and C. M. Lieber, Nature (London) **449**, 885 (2007).
[15] L. Cao, B. Nabet, and J. E. Spanier, Phys. Rev. Lett. **96**, 157402 (2006); S. H. Christiansen, M. Becker, S. Fahlbusch, J. Michler, V. Sivakov, G. Andrä, and R. Geiger, Nanotechnology **18**, 035503 (2007).
[16] E. Stern, J. F. Klemic, D. A. Routenberg, P. N. Wyrembak, D. B. Turner-Evans, A. D. Hamilton, D. A. LaVan, T. M. Fahmy, and M. A. Reed, Nature (London) **445**, 519 (2007).
[17] D. Shiri, Y. Kong, A. Buin, and M. P. Anantram, 2007 International Semiconductor Device Research Symposium, 12–14 December 2007, pp. 1–2.
[18] J. Tersoff, Phys. Rev. B **37**, 6991 (1988).
[19] J. D. Gale and A. L. Rohl, Mol. Simul. **29**, 291 (2003).
[20] J. M. Jancu, R. Scholz, F. Beltram, and F. Bassani, Phys. Rev. B **57**, 6493 (1998); Y. Zheng, C. Rivas, R. Lake, K. Alam, T. B. Boykin, and G. Klimeck, IEEE Trans. Electron Devices **52**, 1097 (2005).
[21] Y. M. Niquet, A. Lherbier, N. H. Quang, M. V. Fernández-Serra, X. Blase, and C. Delerue, Phys. Rev. B **73**, 165319 (2006).
[22] L. Yang, M. P. Anantram, J. Han, and J. P. Lu, Phys. Rev. B **60**, 13874 (1999).
[23] H. Maki, T. Sato, and K. Ishibashi, Nano Lett. **7**, 890 (2007); C. Stampfer, T. Helbling, D. Obergfell, B. Scholberle, M. K. Tripp, A. Jungen, S. Roth, V. M. Bright, and C. Hierold, *ibid.* **6**, 233 (2006).
[24] Y. Ishikawa, K. Wada, D. D. Cannon, J. Liu, H. Chiao Luan, and L. C. Kimerling, Appl. Phys. Lett. **82**, 2044 (2003); J. Menéndez and J. Kouvetakis, *ibid.* **85**, 1175 (2004); R. A. Soref and L. Friedman, Superlattices Microstruct. **14**, 189 (1993).

Downloaded 16 Sep 2008 to 129.97.106.193. Redistribution subject to AIP license or copyright; see http://apl.aip.org/apl/copyright.jsp